THE JOURNAL OF BIOLOGICAL CHEMISTRY VOL. 290, NO. 36, pp. 21915–21924, September 4, 2015

Stanniocalcin-1 Potently Inhibits the Proteolytic Activity of the Metalloproteinase Pregnancy-associated Plasma Protein-A*

Received for publication, March 5, 2015, and in revised form, July 10, 2015 Published, JBC Papers in Press, July 20, 2015, DOI 10.1074/jbc.M115.650143

Søren Kløverpris[‡1], Jakob H. Mikkelsen[‡1], Josefine H. Pedersen[‡], Malene R. Jepsen[‡], Lisbeth S. Laursen[‡], Steen V. Petersen[§], and Claus Oxvig[‡2]

From the [‡]Department of Molecular Biology and Genetics and the [§]Department of Biomedicine, Aarhus University, DK-8000 Aarhus, Denmark

Background: The molecular mechanisms behind previously reported biological effects of stanniocalcin-1 are poorly understood.
Results: Stanniocalcin-1 potently inhibits the proteolytic activity of the metzincin metalloproteinases PAPP-A and PAPP-A2, which promote insulin-like growth factor (IGF) activity in tissues.
Conclusion: Stanniocalcin-1 is a novel proteinase inhibitor.
Significance: Altered stanniocalcin-1 expression may affect IGF signaling *in vivo* under normal or pathological conditions.

Stanniocalcin-1 (STC1) is a disulfide-bound homodimeric glycoprotein, first identified as a hypocalcemic hormone important for maintaining calcium homeostasis in teleost fish. STC1 was later found to be widely expressed in mammals, although it is not believed to function in systemic calcium regulation in these species. Several physiological functions of STC1 have been reported, although many molecular details are still lacking. We here demonstrate that STC1 is an inhibitor of the metzincin metalloproteinase, pregnancy-associated plasma protein-A (PAPP-A), which modulates insulin-like growth factor (IGF) signaling through proteolytic cleavage of IGF-binding proteins (IGFBPs). STC1 potently (K_i = 68 pM) inhibits PAPP-A cleavage of IGFBP-4, and we show in a cell-based assay that STC1 effectively antagonizes PAPP-A-mediated type 1 IGF receptor (IGF1R) phosphorylation. It has recently been found that the homologous STC2 inhibits PAPP-A proteolytic activity, and that this depends on the formation of a covalent complex between the inhibitor and the proteinase, mediated by Cys-120 of STC2. We find that STC1 is unable to bind covalently to PAPP-A, in agreement with the absence of a corresponding cysteine residue. It rather binds to PAPP-A with high affinity (K_D = 75 pM). We further demonstrate that both STC1 and STC2 show inhibitory activity toward PAPP-A2, but not selected serine proteinases and metalloproteinases. We therefore conclude that the STCs are proteinase inhibitors, probably restricted in specificity to the pappalysin family of metzincin metalloproteinases. Our data are the first to identify STC1 as a proteinase inhibitor, suggesting a previously unrecognized function of STC1 in the IGF system.

Stanniocalcin-1 (STC1)[3] is a glycoprotein, first isolated from the corpuscles of Stannius (CS) in teleost fish, where it is known to function as a hypocalcemic hormone important for serum calcium homeostasis (1, 2). STC1 is synthesized in the CS and released from this unique gland in response to elevated serum calcium levels. It negatively regulates calcium ion uptake from the environment via gill ionocytes by regulating the expression of the epithelial calcium ion channel (3, 4). Although the CS or any comparable structure is absent in mammals, mammalian STC1 has been identified (5, 6) and is abundantly expressed in many organs, *e.g.* kidney, heart, lung, liver, adrenal gland, prostate, and ovary (5, 7). However, through the analysis of genetically modified animals, a role of STC1 in mammalian mineral homeostasis has been questioned, in particular because STC1 knock-out mice do not show an altered level of serum calcium compared with wild-type mice (8, 9).

Although STC1 is not believed to affect systemic ion balances in mammals, functions relating to ion transport in isolated cells or in individual organs have been proposed (2). For example, it has been found that STC1 reversibly inhibits transmembrane calcium currents in cardiomyocytes (10), that it inhibits renal phosphate excretion (11), and that it suppresses intestinal calcium absorption (12). Furthermore, mammalian STC1 has been suggested to be involved in physiological processes such as adipogenesis (13), chondrogenesis (14), and development of human cancer (2).

Interestingly, a mammalian homolog of STC1 was discovered more recently and named STC2 (15–17). Although STC2 has been studied less than STC1, it is known to negatively regulate growth, as evidenced by the severe dwarf phenotype of transgenic STC2 mice (18), and also by the increased growth rate of STC2 knock-out mice (9). The molecular mechanism behind this growth-suppressive effect was revealed recently,

* This work was supported by grants from the Lundbeck Foundation, the Novo Nordisk Foundation, and the Danish Council for Independent Research. The authors declare that they have no conflicts of interest with the contents of this article.

Numbering of the amino acid sequences of human STC1 (accession number P52823) (UniProtKB) and STC2 (accession number O76061) (UniProtKB) is according to the full-length proteins.

[1] Both authors contributed equally to this work.
[2] To whom correspondence should be addressed. E-mail: co@mbg.au.dk.

[3] The abbreviations used are: STC, stanniocalcin; IGF, insulin-like growth factor; IGF1R, type 1 IGF receptor; IGFBP, IGF-binding protein; PAPP-A, pregnancy-associated plasma protein-A; PNGase F, peptide *N*-glycosidase F; nt, nucleotide(s); CS, corpuscles of Stannius.

when STC2 was demonstrated to be a proteinase inhibitor of the metzincin metalloproteinase, pregnancy-associated plasma protein-A (PAPP-A) (19).

PAPP-A is a regulator within the insulin-like growth factor (IGF) system (20), and knock-out of the PAPP-A gene in mice causes a severe dwarf phenotype (21), strikingly similar to the phenotype observed upon transgenic overexpression of STC2 (18). IGF-I and -II are ubiquitous polypeptides that exert their effects on cell proliferation and survival by binding to the type 1 IGF receptor (IGF1R) (22). In tissues, the bioavailability of the IGFs is tightly regulated by six homologous IGF-binding proteins (IGFBP-1–6), which function to antagonize receptor activation by high affinity binding of the IGFs. However, proteolytic cleavage of the IGFBPs causes diminished affinity for the growth factors and thus release of bioactive IGF (23). One of the best studied IGFBP proteinases is PAPP-A, which together with its homolog, PAPP-A2 (24), comprises the pappalysin family of the metzincin metalloproteinases (25). PAPP-A is expressed in most tissues (26), and it cleaves IGFBP-4 at a single site in an IGF-dependent manner (27, 28). Additional known substrates of PAPP-A are IGFBP-2 (29) and IGFBP-5 (28).

Thus, STC2 has the potential to silence IGF signaling in tissues where this depends on PAPP-A activity. Curiously, the inhibitory activity of STC2 toward PAPP-A is dependent on the formation of a covalent proteinase·inhibitor complex between PAPP-A and STC2. In agreement with this mechanism, mice transgenic for a variant of STC2, which is unable to bind covalently to PAPP-A, grow like wild-type mice, supporting the interpretation that STC2 reduces IGF signaling through inhibition of PAPP-A (19).

Although STC1 knock-out mice do not show any growth-related phenotype (8), it is interesting that transgenic overexpression of STC1 causes a severe reduction in growth (30), similar to the phenotype of STC2 transgenic mice (18). Based on this observation, we hypothesized that STC1 possesses proteinase inhibitory activity toward PAPP-A.

Experimental Procedures

Plasmid Constructs and Mutagenesis—A plasmid containing the coding sequence of human STC1 (nucleotides (nt) 285-1025 of NM_003155.2 flanked by a 5′ XhoI site and a 3′ HindIII site) were purchased (Invitrogen). The cDNA was cloned into the XhoI/HindIII sites of pcDNA3.1(−)/mycHis A (Invitrogen) to obtain pSTC1. pSTC1(N24Q), pSTC1 (N62Q), and pSTC1(C202A) were constructed by the QuikChange Mutagenesis kit (Agilent Technologies) using pSTC1 as template and the following primer sets: pSTC1(N24Q), 5′-CATGAGGCGGAGCAGCAAGACTCTGTGAGCC-3′ and 5′-GGCTCACAGAGTCTTGCTGCTCCGCCTCATG-3′ (nt 339–369); pSTC1(N62Q), 5′-CTTTTGCATGCCTGGAACAATCCACCTGTGACACAG-3′ and 5′-CTGTGTCACAGGTGGATTGTTCCAGGCATGCAAAAG-3′ (nt 451–486); pSTC1(C202A), 5′-GCAGACAGACCACGCTGCCCAAACACACC-3′ and 5′-GGTGTGTTTGGGCAGCGTGGTCTGTCTGC-3′ (nt 875–913). Plasmid constructs encoding PAPP-A (31), PAPP-A2 (24), STC2 (19), IGFBP-4 (25), and IGFBP-5 (24) were reported elsewhere. Plasmid pSTC2(C211A) was constructed by using the QuikChange kit, pSTC2 (19) as the template, and the following primer set: 5′-CCATCTTGAGCTTCGCCACCTCGGCCATCC-3′ and 5′-GGATGGCCGAGGTGGCGAAGCTCAAGATGG-3′.

Cell Culture and Transfection—Human embryonic kidney 293T cells (293tsA1609neo) were maintained in high-glucose DMEM supplemented with 10% fetal bovine serum, 2 mM glutamine, nonessential amino acids, and gentamicin (Invitrogen). Eighteen hours prior to transfection, 6.0×10^6 cells were plated onto 10-cm culture dishes. The cells were transiently transfected by calcium phosphate coprecipitation using 10–20 μg of plasmid DNA prepared by GenElute HP Plasmid Miniprep Kit (Sigma). Culture supernatants were harvested 48 h post-transfection and cleared by centrifugation, or the cells were further cultured in serum-free medium (CD293, Invitrogen) to facilitate purification.

Protein Purification and Sequence Analysis—Purifications of His-tagged recombinant STC1, STC1(C202A), STC2, IGFBP-4, or IGFBP-5 were carried out by affinity chromatography on a 1-ml HisTrap HP column (GE Healthcare). Serum-free media were diluted 1:1 in 20 mM NaH_2PO_4, 150 mM NaCl, pH 7.4 (PBS), and loaded onto the column with a flow rate of 1 ml/min. The column was washed with 20 column volumes of 50 mM NaH_2PO_4, 1 M NaCl, 20 mM imidazole, 0.05% Tween 20, pH 7.4, followed by 5 column volumes of PBS. The proteins were eluted using 50 mM NaH_2PO_4, 300 mM imidazole, pH 7.4. The eluted STC1 was analyzed by gel filtration on a Superdex 200 Increase 10/300 GL (GE Healthcare). The sample was loaded onto the column with a flow rate of 0.5 ml/min using 20 mM HEPES, 150 mM NaCl, pH 7.4, as running buffer. The eluted fractions (0.5 ml) were analyzed by STC1-specific Western blotting following 12% nonreducing SDS-PAGE. All proteins were dialyzed against 20 mM HEPES, 150 mM NaCl, pH 7.4. IGFBP-4 and IGFBP-5 were further purified by reversed-phase high pressure liquid chromatography (RP-HPLC) on a column (4 × 250 mm) packed with Nucleosil C4 500–7 (Macherey-Nagel), as described previously (24), and radiolabeled (25) using ^{125}I (Amersham Biosciences). Protein purity was assessed by SDS-PAGE, and quantification of purified proteins was done by amino acid analysis. For N-terminal sequence analysis, proteins were separated by reducing SDS-PAGE, blotted onto a PVDF membrane, and Coomassie-stained. Bands were excised, and sequence analysis was performed on an Applied Biosystems 477A sequencer equipped with an online HPLC at levels of ~20 pmol.

Proteinase Assays and Kinetic Analysis—Proteolytic cleavage of IGFBP-4 was performed as previously described (32). Medium harvested from cells transfected with human PAPP-A cDNA were diluted to 20 pM PAPP-A and allowed to preincubate on ice with different concentrations of purified STC1 or STC1(C202A). Proteolytic reactions were initiated by the addition of preincubated ^{125}I-IGFBP-4 (10 nM) and IGF-II (100 nM) (GroPep Bioreagents) in 50 mM Tris-HCl, 100 mM NaCl, 1 mM $CaCl_2$, pH 7.5. Following incubation at 37 °C, the reactions were terminated at various time points by the addition of hot SDS-PAGE sample buffer supplemented with 25 mM EDTA. Substrate and cleavage products were separated by 12% SDS-PAGE, and visualized by autoradiography using a storage phosphorscreen (GE Healthcare) and a Typhoon imaging sys-

tem (GE Healthcare). Band intensities were quantified using the ImageQuant TL 8.1 software (GE Healthcare). Background levels (mock signals) were subtracted, and relative initial velocities (v/v_0) were determined by linear regression assuming no substrate depletion. Determinations of inhibition constants (K_i) were carried out using the Morrison K_i model (competitive inhibition) and GraphPad Prism 5.0 software. In some experiments, media from cells co-transfected with combinations of empty vector, cDNA encoding PAPP-A, cDNA encoding STC1, cDNA encoding STC2, or cDNA encoding STC2(C211A) were diluted 500 times. Proteolytic activity was assessed as described above.

Cleavage of ^{125}I-labeled IGFBP-5 (25, 33) was assessed similarly for the following proteinases with or without a 10-fold molar excess of purified STC1 or STC2: human matrix metalloproteinase-2 (R&D Systems, 902-MP-010), human A disintegrin and metalloproteinase-10 (R&D Systems, 936-AD-020), human matriptase (34), bovine trypsin (Sigma, T-8642), and human PAPP-A2. Enzyme concentrations were 100 nM, except for trypsin (1 μM) and PAPP-A2 (50 pM). Incubation times were 30–180 min.

Western Blotting and Analysis of Potential Covalent Complex Formation—Proteins separated by SDS-PAGE were transferred to a PVDF membrane (Millipore). The membrane was blocked with 2% Tween 20, and equilibrated in 50 mM Tris-HCl, 500 mM NaCl, 0.1% Tween 20, pH 9.0 (TST). Primary antibodies were diluted (to 1–5 μg/ml) in TST containing 0.5% fetal bovine serum and incubated with the membranes overnight at room temperature. The following primary antibodies were used: rabbit polyclonal anti-human PAPP-A (35), goat polyclonal anti-STC1 (R&D Systems, AF2958), goat polyclonal anti-STC2 (R&D Systems, AF2830), mouse monoclonal PY99 (Santa Cruz Biotechnology, sc-7020) for the detection of phosphotyrosine residues, mouse monoclonal CT-1 (GroPep Bioreagents, MAJ1) for the detection of human IGF-I receptor, or mouse monoclonal AC-74 (Sigma, A5316) for the detection of β-actin. The membranes were incubated for 1 h at room temperature with one of the following secondary antibodies diluted 1:2000 in TST containing 0.5% fetal bovine serum: polyclonal swine anti-rabbit IgG-HRP (DAKO, P0217), polyclonal rabbit anti-goat IgG (DAKO, P0449), or polyclonal rabbit anti-mouse IgG-HRP (DAKO, P0260). Between steps, the membrane was washed in TST. The blots were developed using enhanced chemiluminescence (ECL Prime, GE Healthcare), and images were captured using an ImageQuant LAS 4000 instrument (GE Healthcare) and analyzed using the ImageQuant TL 8.1 software (GE Healthcare).

To probe for potential covalent complex formation between PAPP-A and STCs, culture supernatants from cells transfected with cDNA encoding PAPP-A were mixed with culture supernatants from cells transfected with pSTC1 or pSTC2 and incubated for 0–16 h at 37 °C. In another experiment, cells were co-transfected with cDNA encoding PAPP-A and empty vector, cDNA encoding STC2, or cDNA encoding STC2(C211A). Afterward, the proteins were separated by nonreducing 3–8% SDS-PAGE and analyzed by PAPP-A Western blotting as described above.

Mass Spectrometry—Purified STC1 was boiled for 10 min in TBS containing 0.2% (w/v) RapiGest (Waters) and 2 mM iodoacetamide. The sample was allowed to cool, trypsin was added at a 1:20 ratio (w/w), and the sample was incubated overnight at 37 °C. The sample was acidified by the addition of TFA (1% (v/v) final), and the generated peptides were separated by reversed-phase UPLC using a BEH300 C18 column (2.1 mm × 15 cm; 1.7 μm) operated by an Acquity UPLC system (Waters). The column was developed at a flow rate of 300 μl/min using a linear gradient of 90% acetonitrile, 0.08% (v/v) TFA (solvent B) in 0.1% (v/v) TFA (solvent A) (1%/min). Peptides were detected by absorption at 220 nm and collected manually. Both the unfractionated digest and the collected peptides were analyzed by MALDI mass spectrometry using an Autoflex III instrument (Bruker Daltonics) operated in positive mode. The matrices used for analysis were either α-cyano-4-hydroxycinnamic acid prepared in 70% (v/v) acetonitrile, 0.1% (v/v) TFA acid, or 2,5-dihydroxyacetophenone prepared in 20 mM diammonium hydrogen citrate, 75% (v/v) ethanol. The instrument was operated in reflector mode and calibrated in the mass range of 1000 to 3200 Da using a peptide calibration standard (Bruker Daltonics). When appropriate, MALDI spectra were evaluated by using the GPMAW software (Lighthouse Data). Peptides selected for further analysis were lyophilized, resuspended in PBS, and subsequently reduced by the addition of 10 mM DTT or deglycosylated by the addition of PNGase F (Roche Applied Science). The peptides were subsequently recovered by using C18 Stage Tips (Thermo) and eluted directly onto the MALDI target using the appropriate matrix solution.

Surface Plasmon Resonance Analysis—Surface plasmon resonance experiments were carried out on a Biacore T200 (GE Healthcare). Using amine coupling, purified monoclonal antibody 234-5 (36) was immobilized in flow cells (FC) 3 and 4 of a Series S CM5 Sensor Chip (GE Healthcare). To reach a coupling density of 5,000 response units, the antibody was diluted to 30 μg/ml in 10 mM sodium acetate, pH 4.75. The remaining active groups were blocked by a 7-min injection of 1 M ethanolamine, pH 8.0. For data collection, recombinant human PAPP-A (350 response units) in culture medium was captured in FC4 only, using FC3 as a reference cell. A 2-fold serial dilution (6.25 nM to 195 pM) of purified recombinant human STC1 in 10 mM HEPES, pH 7.5, 150 mM NaCl, 1 mM $CaCl_2$, and 0.05% Tween 20, was injected over both FCs at 30 μl/min. The association phase was 180 s, followed by a 1,000-s dissociation phase. At the end of each binding cycle, both surfaces were regenerated by a 40-s injection of 0.1 M glycine, pH 2.5, and 0.5 M guanidine hydrochloride. Analyte (STC1) concentration was determined by amino acid analysis. Binding analysis was performed at 25 °C, and data were collected at a rate of 10 Hz. Recorded signals were subtracted the background signal, as determined by the response obtained from the reference cell. Global fitting of a 1:1 Langmuir model was performed, using Biacore T200 Evaluation Software, version 1.0.

IGF Receptor (IGF1R) Stimulation Assay—The assay was carried out as previously described in detail (37). Briefly, cells stably expressing the type 1 IGF receptor (IGF1R), 293-IGFR (clone H), were starved and rinsed in PBS containing 0.1 mg/liter of $CaCl_2$ and 0.1 mg/liter of $MgCl_2$. The starved cells were

stimulated with combinations of IGF-I (10 nM), IGFBP-4 (50 nM), PAPP-A (2.5 nM), and STC1 (15 nM) for 15 min. Prior to stimulation, IGF-I and IGFBP-4 were incubated for 20 min at 37 °C in 20 mM HEPES, 100 mM NaCl, 1 mM $CaCl_2$, pH 7.4, to allow the IGF-I·IGFBP-4 complex to form. Then PAPP-A, preincubated with or without STC1, was added, and cleavage reactions were carried out at 37 °C for 20 min in the same buffer. Following stimulation, the cells were lysed for 10 min on ice with RIPA buffer (Sigma, R0278), supplemented with Proteinase Inhibitor Mixture (Sigma, P8340) and Phosphatase Inhibitor Mixture Set II (EMD Millipore, 524625). β-Subunit phosphorylation of the IGF1R was quantified by Western blotting of cleared and reduced lysates using mAb PY99, and total IGF1R was quantified similarly using mAb CT-1. For loading controls, blots were stripped and reprobed with actin mAb AC-74. Band intensities were quantified using ImageQuant TL 8.1 software (GE Healthcare). The signals of mAb PY99 were plotted and analyzed using the GraphPad Prism 5.0 software. Statistical analysis was performed using one-way analysis of variance followed by Dunnett's test.

Results

STC1 Inhibits the Proteolytic Activity of PAPP-A —To test the hypothesis that STC1 is a proteinase inhibitor of PAPP-A, proteolytic activity toward IGFBP-4 in culture media of cells transfected with PAPP-A cDNA alone or in combination with STC1 cDNA was assessed (Fig. 1*A*). In culture media containing PAPP-A alone, IGFBP-4 was cleaved at a single site resulting in two co-migrating cleavage products. However, no activity was detected in the culture medium following co-transfection with STC1 cDNA, although comparable levels of PAPP-A expression were apparent by Western blotting (Fig. 1*B*). These data indicate that STC1 is capable of inhibiting the proteolytic activity of PAPP-A.

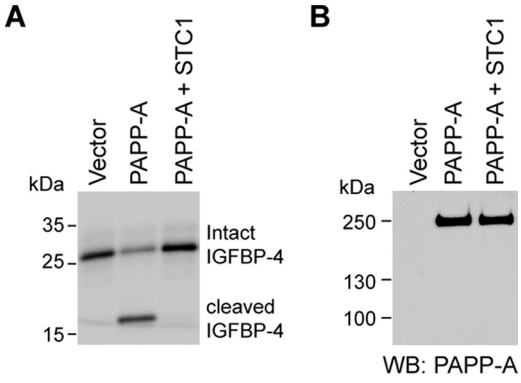

FIGURE 1. **Co-transfection with cDNA encoding stanniocalcin-1 abrogates the proteolytic activity of PAPP-A.** *A*, PAPP-A proteolytic activity toward radiolabeled IGFBP-4 in culture media from HEK293T cells transfected with the indicated combinations of cDNAs. Cleavage of IGFBP-4 by PAPP-A followed by separation in SDS-PAGE (12%) results in the generation of two co-migrating cleavage products of ~16 kDa. *B*, PAPP-A Western blot (*WB*) following reducing 3–8% SDS-PAGE of culture supernatants from *A*.

Analysis of STC1 Heterogeneity—Prior to further characterization of the inhibitory potential of STC1, recombinant STC1 was affinity purified from culture medium of transfected HEK293T cells and analyzed by SDS-PAGE (Fig. 2*A*). Reduced STC1 migrated as a band above 35 kDa, and Edman degradation of the reduced protein revealed two N-terminal sequences, corresponding to cleavage at Ala-(17)–Thr-4 and Glu-(20)–Ala (Fig. 2*A*). In non-reducing SDS-PAGE, two species of STC1 in approximately equal amounts were observed (Fig. 2*A*). One species migrated corresponding to a dimer of ~80 kDa, and the other migrated as a monomer of ~35 kDa. In gel filtration, the protein eluted as two overlapping peaks, suggesting that a fraction of the protein is actually monomeric in solution (Fig. 2*B*). To validate the integrity of the protein, we analyzed the disulfide pairing by subjecting tryptic peptides separated by reversed-phase chromatography to MALDI mass spectrometry (Table 1). Determined masses of isolated peptides are in agreement with the previously published data on the disulfide structure of human (38) and salmon (39) STC1, for which five intramolecular bonds (Cys-45–Cys-59, Cys-54–Cys-74, Cys-65–Cys-114, Cys-98–Cys-128, and Cys-135–Cys-170) and one intermolecular bond (Cys-202–Cys-202) were demonstrated. However, we also identified a peptide containing a cysteinylated variant of Cys-202 (Table 1 and Fig. 3*A*). Cysteinylation of Cys-202 is likely to prevent formation of the interchain disulfide bond responsible for covalent dimerization and thus explains that a fraction of the protein migrates as a monomer in non-reducing SDS-PAGE.

Furthermore, we identified a peptide containing a carbohydrate-substituted variant of Asn-62 (Fig. 3*B*). Based on the observed peptide masses, the carbohydrate moiety is a complex-type core fucosylated triantennary structure with no terminal sialylation. In agreement with this interpretation, neuraminidase treatment did not affect the peptide mass (not

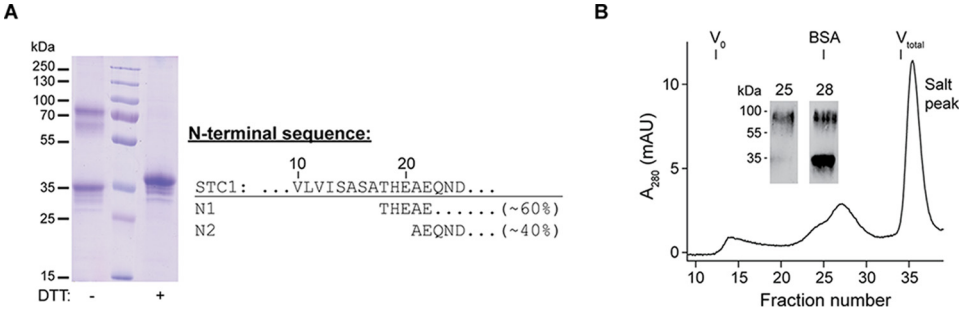

FIGURE 2. **N-terminal sequence analysis and analytical gel filtration of purified STC1.** *A*, Coomassie-stained 12% SDS-PAGE gel of purified STC1 under nonreducing (−) or reducing (+) conditions. N-terminal sequences (*N1* and *N2*) determined by Edman degradation of reduced STC1 are aligned with the amino acid sequence of STC1 including the signal peptide. *B*, analytical gel filtration of purified STC1. Positions of the salt peak, the void volume (V_0), the total volume (V_t), and the elution position of bovine serum albumin (*BSA*, 66 kDa) are indicated. STC1 Western blotting of selected fractions following nonreducing 12% SDS-PAGE is shown.

TABLE 1

MALDI mass spectrometry of tryptic peptides derived from purified human STC1

Average masses are indicated by asterisks.

Experimental mass[a]	Calculated mass	Peptide	Modification
m/z			
6118.0*	6117.5*	Cys–45–Lys–75	*N*–Linked glycan: Asn–62
		Cys–114–Arg119	Disulfide bonds[b]: Cys–45–Cys–59, Cys–54–Cys–74, Cys–65–Cys–114
3979.7	3979.6	Cys–45–Lys–75	No *N*–linked glycan of Asn–62
		Cys–114–Arg–119	Disulfide bonds[b]: Cys–45–Cys–59, Cys–54–Cys–74, Cys–65–Cys–114
5172.2*[c]	5172.5*	Ile–186–Arg–208	Disulfide bond:
			Dimerization via Cys–202
2706.2[c]	2706.3	Ile–186–Arg–208	Cysteinylation of Cys–202
2319.9	2319.1	Cys–98–Lys–106	Disulfide bond:
		Met–120–Lys–131	Cys–98–Cys–128
2426.0	2425.2	Leu–132–Lys–139	Disulfide bond:
		Ser–166–Arg–179	Cys–135–Cys–170

[a] Experimental masses were obtained in reflector mode (monoisotopic) or linear mode (average).
[b] The listed disulfide bonds are based on Ref. 38.
[c] Spectra of indicated peptides are shown in Fig. 3*A*.

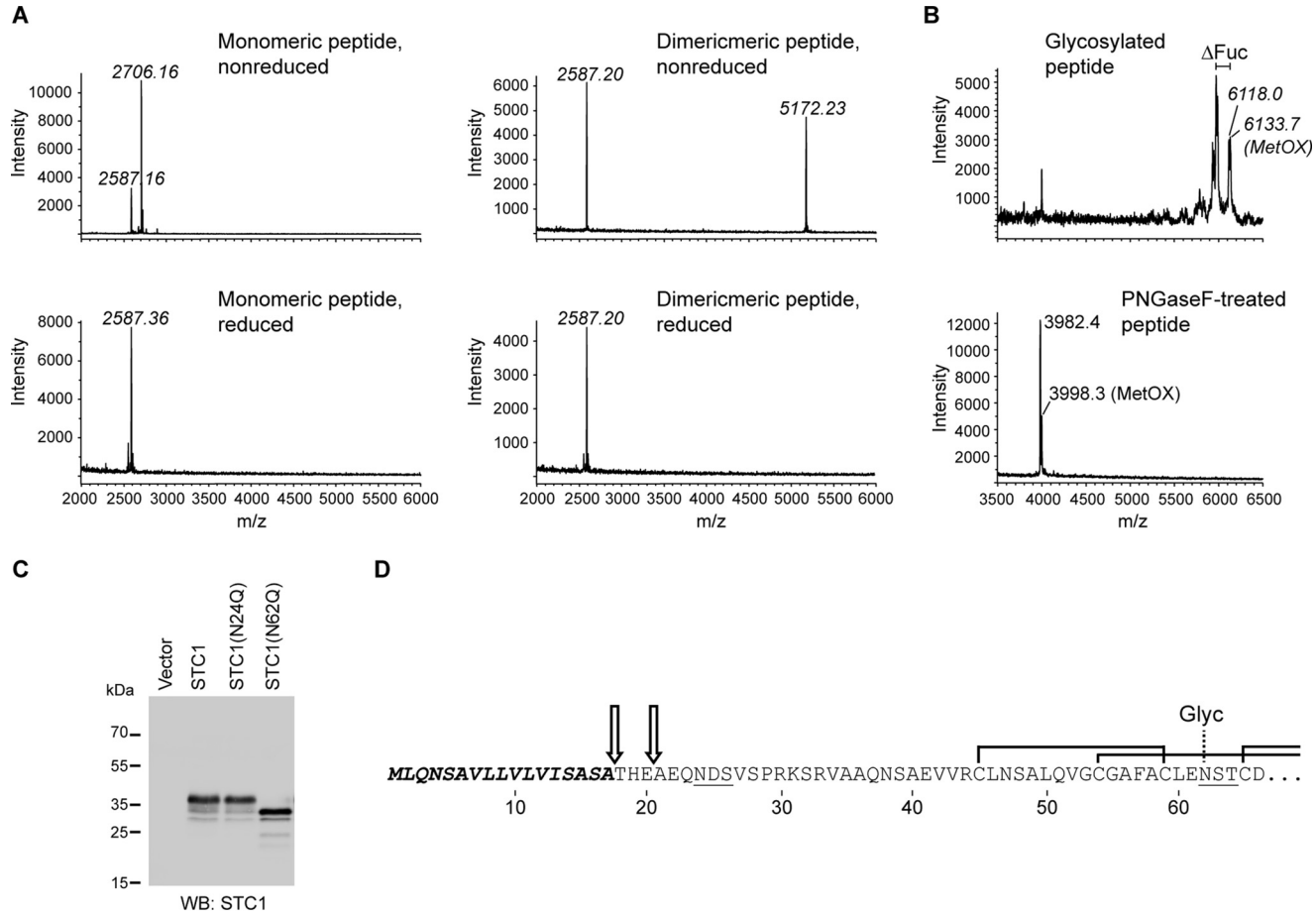

FIGURE 3. **Analysis of peptides derived from purified STC1.** *A*, MALDI mass spectra of STC1 peptides containing Cys-202. The *upper-left panel* shows the monomeric Ile-186–Arg-208 peptide, in which Cys-202 is cysteinylated. Reduction (*lower-left panel*) causes a loss of 118.8 Da, corresponding to the loss of a cysteine residue. The *upper-right panel* shows the dimeric Ile-186–Arg-208 peptide (of 5172.23 Da), in which Cys-202 is engaged in forming the interchain disulfide bond, responsible for covalent dimerization of the intact STC1. Following reduction (*lower-right panel*), all of the peptide is present in the monomeric form. *B*, MALDI mass spectra of the STC1 peptide containing Asn-62 before (*upper panel*) and after (*lower panel*) treatment with PNGase F. Masses of the peptides are shown and the loss of a fucose monosaccharide moiety is indicated (Δ*Fuc*). A fraction of the peptide contains an oxidized methionine residue (*MetOX*). *C*, STC1 Western blot following 12% reducing SDS-PAGE of culture supernatants from cells transfected with cDNA encoding STC1 variants, in which the asparagine residues (Asn-24 and Asn-62) of the two potential *N*-glycosylation sites are substituted individually with a glutamine residue. *D*, the N-terminal amino acid sequence of STC1 with the two observed signal peptidase cleavage sites indicated by *arrows*. Disulfide bonds are shown as *black lines*, and the two potential *N*-glycosylation sites are *underlined*, one of which was demonstrated to be substituted with carbohydrate (*Glyc*).

shown), whereas complete deglycosylation of the peptide was obtained by treatment with PNGase F (Fig. 3*B*). We also identified a non-glycosylated variant of the peptide containing Asn-62 (Table 1), in agreement with the heterogeneity of the protein as evident by SDS-PAGE analysis (Fig. 2). Concordantly, Western blot analysis of a mutated variant of STC1, STC1(N62Q), in which Asn-62 is substituted for a glutamine residue, showed a reduction in molecular mass (Fig. 3*C*), in fair agreement with the loss of the *N*-linked glycan. One other asparagine residue (Asn-24) of STC1 is predicted to be subject

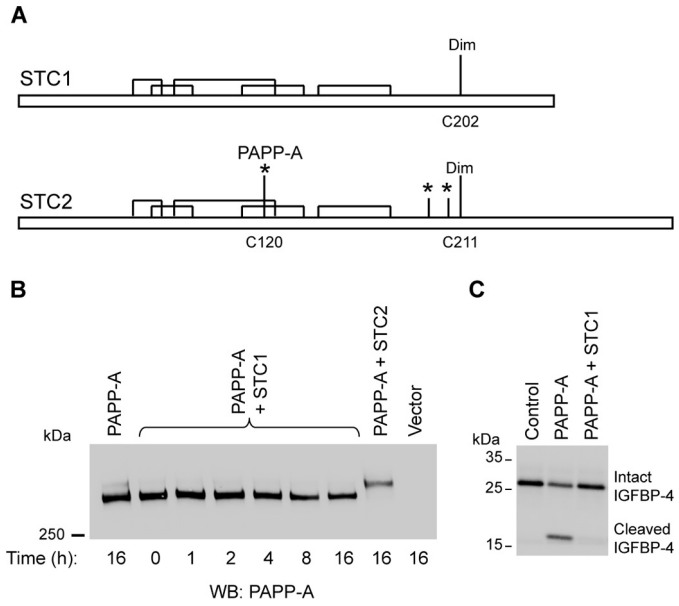

FIGURE 4. **Unlike STC2, STC1 forms a noncovalent inhibitory complex with PAPP-A.** *A*, schematic representations of the previously reported disulfide structure of STC1 (38) and the predicted disulfide structure of STC2. Disulfide bonds are shown as *black lines*. The positions of cysteine residues engaged in interchain disulfide bond formation are indicated (*Dim*) and *asterisks* indicate positions of three cysteines of STC2, which have no counterpart in STC1. The position of Cys-120 of STC2, which is required for formation of the PAPP-A·STC2 complex (19), is indicated (PAPP-A). *B*, PAPP-A Western blot following 3–8% nonreducing SDS-PAGE of culture supernatants from cells transfected with cDNA encoding PAPP-A incubated 0–16 h with medium from cells transfected with empty vector, STC1 cDNA, or STC2 cDNA. Note that the migration of PAPP-A is not affected by prolonged incubation with STC1, whereas all of PAPP-A has formed a covalent complex of higher molecular mass following incubation for 16 h with STC2. *C*, proteolytic activity toward radiolabeled IGFBP-4 in culture media from cells transfected with PAPP-A cDNA in the presence or absence of a 10-fold molar excess of purified STC1. PAPP-A and STC1 was not preincubated prior to the cleavage reaction.

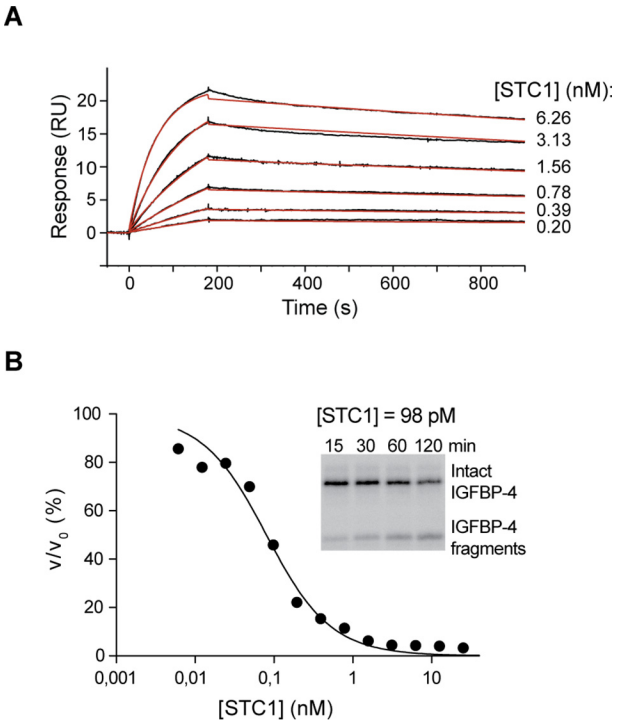

FIGURE 5. **STC1 is a high affinity inhibitor of PAPP-A.** *A*, surface plasmon resonance analysis of STC1 binding to PAPP-A. 2-Fold serial dilutions of STC1 were injected over a surface with or without antibody-captured PAPP-A. Recorded binding curves are shown in *black*, and a global 1:1 Langmuir fit is shown in *red*. The fitted constants are: $k_a = 2.78 \pm 0.001 \times 10^6$ M^{-1} s^{-1} and $k_d = 2.08 \pm 0.004 \times 10^{-4}$ s^{-1}, resulting in $K_D = 7.5 \times 10^{-11}$ M. The sensorgrams are truncated, but all collected data points were used for model fitting. *B*, kinetic analysis of STC1 inhibition of PAPP-A-mediated IGFBP-4 cleavage. Relative initial velocities (v/v_0) of PAPP-A-mediated IGFBP-4 cleavage in the presence of increasing concentrations of STC1 are shown. The inhibition constant (K_i) was determined to be $6.8 \pm 0.7 \times 10^{-11}$ M by fitting the Morrison K_i model (competitive inhibition) to the data.

to *N*-linked glycosylation. However, based on peptide masses (not shown) and mutational analysis (Fig. 3*C*), this residue is not substituted with carbohydrate.

In summary, the preparation of purified STC1 is a mixture of homodimeric and monomeric protein. The STC1 subunit is partially glycosylated at Asn-62, and N-terminal sequence analysis showed two sequences, different by 3 amino acids, indicating the presence of two signal peptidase cleavage sites (Fig. 3*D*). The co-existence of STC1 monomers and covalent dimers has also been observed following expression in CHO cells (54). It is interesting that previous analyses of recombinant STC1 has been based on preparations subjected to various chromatographic procedures that might cause separation of the two species (38, 40).

STC1 Inhibition of PAPP-A Is Based on Noncovalent High Affinity Interactions—We previously demonstrated that inhibition of PAPP-A by STC2 requires formation of a covalent PAPP-A·STC2 complex, which can be formed *in vitro* by coincubating separately synthesized PAPP-A and STC2 (19). The slower migration of PAPP-A following complex formation with STC2 can be demonstrated using Western blotting following separation of the proteins by nonreducing SDS-PAGE. Interestingly, formation of the PAPP-A·STC2 complex depends on Cys-120 of STC2, which is not conserved in the amino acid sequence of STC1 (Fig. 4*A*). In agreement with this observation, a covalent complex between PAPP-A and STC1 could not be detected by Western blotting when the two components were incubated for up to 16 h (Fig. 4*B*). Still, however, the addition of STC1 to PAPP-A caused efficient inhibition of IGFBP-4 cleavage without any preincubation (Fig. 4*C*), showing that inhibition of PAPP-A by STC1 does not involve covalent complex formation.

For quantitative assessment of noncovalent interactions between STC1 and PAPP-A, we analyzed the binding of STC1 to immobilized PAPP-A by surface plasmon resonance, and the inhibitory properties of STC1 toward PAPP-A using IGFBP-4 as a substrate. The dissociation constant (K_D) was determined to be 75 pM (Fig. 5*A*), and concordantly, the inhibition constant (K_i) of STC1 was determined to be 68 pM (Fig. 5*B*). These results might be biased because not all of STC1 is present as a covalent dimer (Fig. 2). We therefore expressed and purified a mutated variant of STC1, STC1(C202A), in which the cysteine residue forming the Cys-202–Cys-202 interchain disulfide bridge is mutated to an alanine residue. The inhibition constant of STC1(C202A) was determined to be 5–10-fold higher compared with that of wild-type STC1 (data not shown), and therefore, the inhibitory potential of the covalent STC1 dimer may be slightly underestimated. It should be noted, however, that the wild-type STC1 monomer and STC1(C202A) may differ

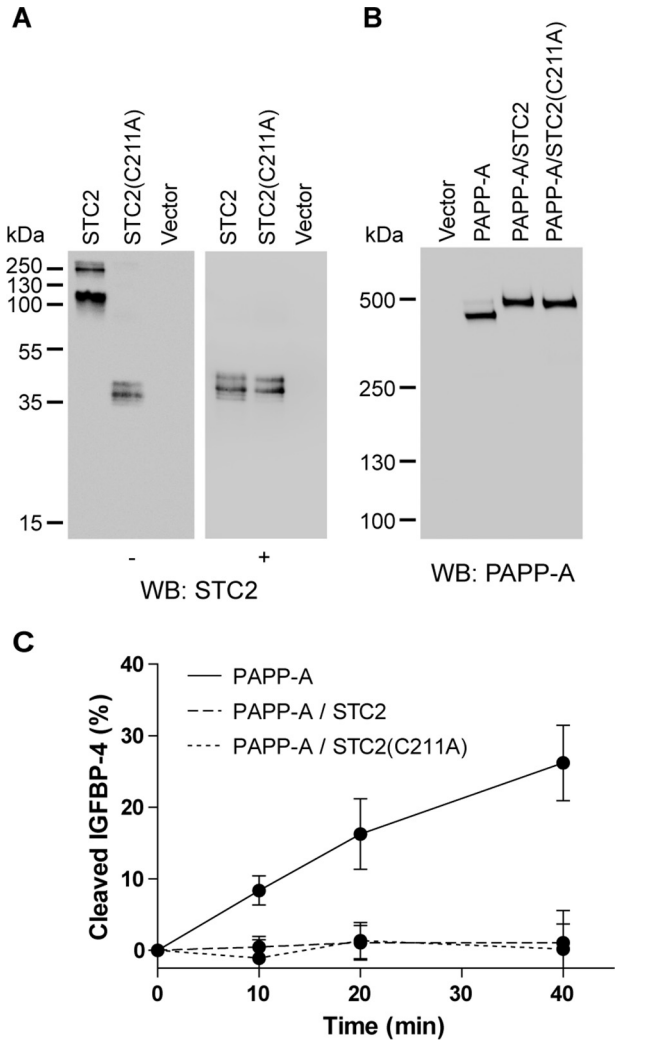

FIGURE 6. **Covalent dimerization of STC2 is not required for inhibition of PAPP-A.** *A*, STC2 Western blot (*WB*) following nonreducing (−) or reducing (+) 12% SDS-PAGE of culture supernatants from cells transfected with empty vector, cDNA encoding STC2, or cDNA encoding STC2(C211A). *B*, PAPP-A Western blot following nonreducing 3–8% SDS-PAGE of culture supernatants from cells co-transfected with PAPP-A cDNA and empty vector, cDNA encoding STC2, or cDNA encoding STC2(C211A). *C*, PAPP-A proteolytic activity toward IGFBP-4 in medium from cells co-transfected with PAPP-A cDNA and empty vector, STC2 cDNA, or STC2(C211A) cDNA. Results are mean ± S.D. from four independent experiments.

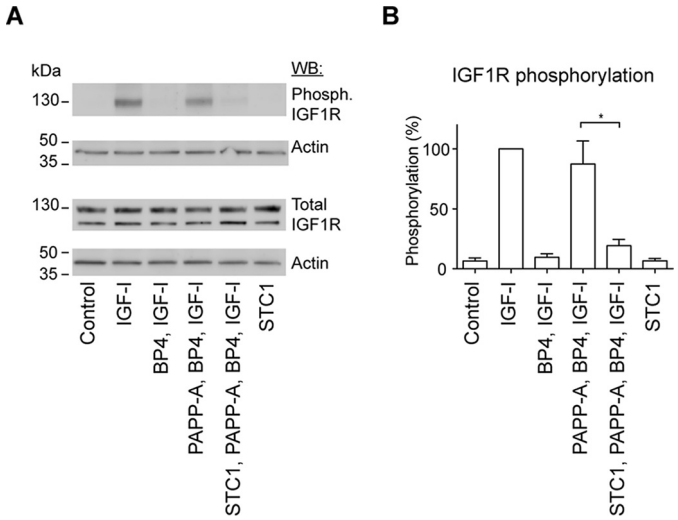

FIGURE 7. **STC1 inhibits IGF signaling *in vitro*.** *A*, cells stably expressing the IGF1R was stimulated with combinations of IGF-I, IGFBP-4 (BP4), PAPP-A, and STC1. Phosphorylated and total IGF1R were detected in cell lysates by Western blotting (*WB*). β-Actin was used as loading control. *B*, the IGF1R phosphorylation was quantified from the Western blots and normalized to the signal with IGF alone. Results are mean ± S.D. from four independent experiments (*ns*, not statistically significant; *, $p < 0.0001$).

structurally, in particular at the dimerization interphase because Cys-202 of the wild-type protein is cysteinylated.

Based on these results, we conclude that STC1 is a proteinase inhibitor of PAPP-A, which, unlike STC2, does not require covalent complex formation. Rather, its potent inhibitory activity is based on a high-affinity interaction between STC1 and PAPP-A.

Upon recombinant expression, all of STC2 exists as disulfide-linked dimers (19). To delineate whether the covalent linkage between the STC2 subunits is required for inhibition of the proteolytic activity of PAPP-A, a variant of STC2 in which the dimerization cysteine (Cys-211) was substituted for alanine was expressed in HEK293T cells. Culture media from transfected cells were analyzed by Western blotting, confirming that this variant, STC2(C211A), is unable to form a covalent dimer (Fig. 6*A*). To first determine whether STC2(C211A) is able to interact covalently with PAPP-A, HEK293T cells were co-transfected with cDNA encoding PAPP-A, and cDNA encoding STC2 or STC2(C211A). PAPP-A-specific nonreducing Western blotting of media from transfected cells shows that a complex that migrates like the wild-type covalent PAPP-A·STC2 complex (19) is formed (Fig. 6*B*). Thus, although STC2(C211A) is unable to dimerize covalently when expressed alone, it apparently is able to covalently complex with PAPP-A. We then tested the inhibitory activity of STC2(C211A) toward PAPP-A using IGFBP-4 as a substrate. Like wild-type STC2, STC2(C211A) fully inhibits the proteolytic activity of PAPP-A (Fig. 6*C*), showing that covalent dimerization of STC2 is not necessary for inhibition. These results do not allow any conclusions about reaction kinetics to be made; it is possible that the reaction between PAPP-A and wild-type STC2 is faster than the reaction between PAPP-A and STC2(C211A).

Because of the noncovalent binding between STC1 and PAPP-A, similar gel-based analysis of the complex formation (Fig. 6*B*) cannot be carried out for STC1. However, because STC1 and STC2 are homologous proteins with similar inhibitory specificities, it is reasonable to speculate that STC1 forms a similarly composed complex with PAPP-A, although current data do not allow a prediction of the relevant stoichiometries.

STC1 Inhibits IGF Signaling in Vitro—Because PAPP-A is known to regulate the bioavailability of IGFs through proteolytic cleavage of IGFBPs, a cell based assay was used to test the effect of STC1 on IGF signaling (37). Cells overexpressing the IGF type 1 receptor (IGF1R) were stimulated with IGF-I preincubated with the indicated components (Fig. 7*A*), and the degree of IGF1R phosphorylation was quantified based on Western blotting (Fig. 7*B*). In the presence of IGFBP-4, no receptor stimulation was observed, whereas addition of PAPP-A leads to regained IGF1R phosphorylation (37). When STC1 was also added, receptor phosphorylation was markedly reduced again. These experiments demonstrate the potential of STC1 to modulate the bioavailability of IGF and hence IGF signaling.

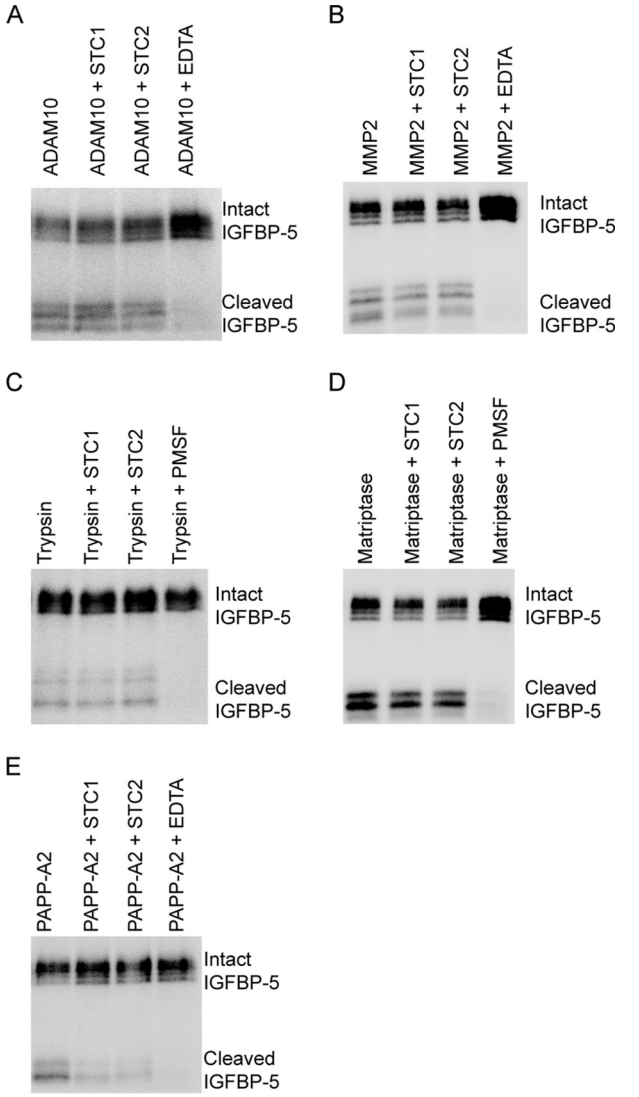

FIGURE 8. **STC1 and STC2 inhibit the pappalysins (PAPP-A and PAPP-A2).** Proteolytic activity toward radiolabeled IGFBP-5 was assessed. The experiments were carried out in the absence or presence of STC1, STC2, or a general proteinase inhibitor (EDTA or PMSF). The following proteinases were analyzed: *A*, A disintegrin and metalloproteinase (*ADAM*)-10; *B*, matrix metalloproteinase-2 (*MMP2*); *C*, trypsin; *D*, matriptase; *E*, PAPP-A2.

STC1 and STC2 Are Inhibitors of the Pappalysins—Having established STC1 and its homolog, STC2, as novel proteinase inhibitors of PAPP-A, we assessed their inhibitory activity toward a panel of other proteinases, representing both metalloproteinases and serine proteinases. We used a radiolabeled native protein substrate, IGFBP-5, which can be cleaved by many proteolytic enzymes (Fig. 8). Prior to the addition of substrate, the proteinases were incubated for 8 h with the STCs to allow potential covalent bond formation. However, neither STC1 nor STC2 showed inhibitory activity toward A disintegrin and metalloproteinase-10, matrix metalloproteinase-2, trypsin, or matriptase (Fig. 8, *A–D*). In contrast, the activity of PAPP-A2 was inhibited by both STC1 and STC2 (Fig. 8*E*). PAPP-A and PAPP-A2 are homologous proteins, together comprising the pappalysin family of the metzincin metalloproteinases (25). From these data, we therefore conclude that STC1 and STC2 are proteinase inhibitors of the pappalysins.

Discussion

We have established STC1 as a novel proteinase inhibitor of the metzincin metalloproteinase PAPP-A, and we have shown that the inhibitory activity of STC1 is based on high affinity interactions between the proteinase and the inhibitor. This is in contrast to the homolog STC2, which is dependent on the formation of a covalent complex for inhibition of PAPP-A (19). We have also shown that STC1 is able to inhibit IGF signaling *in vitro* through silencing of PAPP-A activity. Finally, we have demonstrated that PAPP-A2, the other member of the pappalysin family of metalloproteinases, can be inhibited by both STC1 and STC2. In contrast, neither STC1 nor STC2 showed inhibitory activity toward other selected metzincin metalloproteinases or serine proteinases.

Secondary structure predictions and circular dichroism spectroscopy indicate that both STC1 and STC2 have a high α-helical content (19, 38), but no known modules or motifs can be recognized in the amino acid sequences. Therefore, the inhibitory function of the proteins is surprising and could not have been predicted. The degree of sequence identity between STC1 and STC2 is relatively low, and hence the conserved pattern of cysteine residues is important for defining the STCs, particularly relevant for evolutionary distant species (41). Comparison of the human STCs shows that the region contained between the first (Cys-45) and the 10th (Cys-170) cysteine of STC1, containing all intrachain disulfide bridges (see Fig. 4*A*), has a sequence identity of 39%. The C-terminal portion of the proteins are less conserved, and STC2 contains an extended sequence stretch of more than 40 residues with no counterpart in STC1 (41). This indicates that structural features important for the common inhibitory function of STC1 and STC2 lie within a core region of 126 residues, containing a total of five intrachain disulfide bonds.

The covalent complex between STC2 and PAPP-A, which is proteolytically inactive, forms *in vitro* over hours and requires Cys-120 of STC2. In fact, substitution of this cysteine residue for an alanine causes loss of inhibitory activity toward PAPP-A (19). In agreement with the absence of a corresponding cysteine residue in its sequence, STC1 binds PAPP-A noncovalently but with high affinity (K_D = 75 pM). Concordantly, kinetic analysis showed that STC1 potently (K_i = 68 pM) inhibits PAPP-A and therefore has the potential to be a physiological regulator of PAPP-A activity and hence IGF signaling *in vivo*. For comparison, the physical interaction between STC1 and PAPP-A is comparable in strength to some of the high affinity interactions between many well characterized pairs of the tissue inhibitors of metalloproteinases and their target proteinases (42).

Is there any evidence to suggest a functional connection between the role of STC1 as a proteinase inhibitor of PAPP-A and other possible biological activities of STC1? In teleost fish, STC1 inhibits uptake of calcium ions from the environment through the gills (3), and recently, studies in zebrafish have revealed that this involves regulated expression of the epithelial calcium ion channel in gill ionocytes (43, 44), although some molecular details are still lacking. In this regard, it is interesting that an apparent link between calcium levels and IGF-induced cell proliferation has been demonstrated for zebrafish skin

ionocytes, which have a similar regulatory role in the embryo before the gills are developed: activation of IGF1R-PI3K-Akt signaling was found to result from low levels of extracellular calcium ions (45). The proposed signaling mechanism involves zebrafish IGFBP-5, which is also a PAPP-A substrate (46). Although speculative, STC1 and PAPP-A may therefore in some cells or tissues be functionally connected in the network of proteins regulating transepithelial calcium ion uptake, possibly also relevant in mammals (4).

Based on overexpression studies in mice, it is fair to assume that not only STC2 (18, 19) but also STC1 (30) can function as inhibitors of PAPP-A and PAPP-A2 *in vivo*. The two pappalysins and the STCs are ubiquitously expressed in many human tissues and we therefore suggest that functional interactions occur *in vivo*, which is likely to affect IGF signaling locally in both human health and disease. For example, increased IGF signaling has consistently been linked to several aspects of human cancer development (47). For this reason, it is no surprise to find that expression of PAPP-A is up-regulated in several different types of cancer (20) and has in fact proved useful in animal models as a target to indirectly inhibit IGF signaling (48, 49). Many studies link STC1 and STC2 to different aspects of human cancer, in particular metastasis (50). Although some studies report a loss of STC expression, *e.g.* in breast cancer as a consequence of lost BRCA1 activity (51), the majority of these studies report increased levels of expression (2, 52). This is in apparent conflict with a role of the STCs as inhibitors of PAPP-A and hence IGF signaling. On the other hand, a recent paper reported that breast cancer cells become more invasive following down-regulation of PAPP-A (53). Because the STCs have not previously been connected to PAPP-A or other components of the IGF system, they have been considered to represent different biological systems and therefore been studied separately. Future studies are required to address the raised questions. In particular, distinction between tumor stages and between individual cells of the tumor microenvironment may lead to a better understanding of how these molecules function together.

Overall, we have shown that STC1 is a proteinase inhibitor of the pappalysins, and we hypothesize that STC1 is a relevant modulator of the IGF system in human physiology. However, whereas this hypothesis has a solid biochemical rationale, it is also possible that the pappalysins have modulatory effects on functions of the stanniocalcins, which may be unrelated to IGF signaling. This hypothesis should also be tested.

Author Contributions—S. O. K., J. H. M., and C. O. conceived and coordinated the study. S. O. K. contributed with experiments of Figs. 1, 2, 4, and 6–8. J. H. M. carried out experiments of Figs. 5 and 8. J. H. P. carried out experiments of Fig. 6. M. R. J. carried out preliminary experiments. L. S. L. carried out experiments of Fig. 7. S. V. P. carried out experiments of Fig. 3. S. O. K. and C. O. wrote the paper. All authors reviewed the results and approved the final version of the manuscript.

Acknowledgments—We thank Sanne N. Andersen for technical assistance, and Jan K. Jensen for the kind gift of recombinant human matriptase.

References

1. Wagner, G. F., Hampong, M., Park, C. M., and Copp, D. H. (1986) Purification, characterization, and bioassay of teleocalcin, a glycoprotein from salmon corpuscles of Stannius. *Gen. Comp. Endocrinol.* **63,** 481–491
2. Yeung, B. H., Law, A. Y., and Wong, C. K. (2012) Evolution and roles of stanniocalcin. *Mol. Cell. Endocrinol.* **349,** 272–280
3. Wagner, G. F., and Dimattia, G. E. (2006) The stanniocalcin family of proteins. *J. Exp. Zool. A Comp. Exp. Biol.* **305,** 769–780
4. Hwang, P. P., and Chou, M. Y. (2013) Zebrafish as an animal model to study ion homeostasis. *Pflugers Arch.* **465,** 1233–1247
5. Chang, A. C., Janosi, J., Hulsbeek, M., de Jong, D., Jeffrey, K. J., Noble, J. R., and Reddel, R. R. (1995) A novel human cDNA highly homologous to the fish hormone stanniocalcin. *Mol. Cell. Endocrinol.* **112,** 241–247
6. Olsen, H. S., Cepeda, M. A., Zhang, Q. Q., Rosen, C. A., Vozzolo, B. L., and Wagner, G. F. (1996) Human stanniocalcin: a possible hormonal regulator of mineral metabolism. *Proc. Natl. Acad. Sci. U.S.A.* **93,** 1792–1796
7. Varghese, R., Wong, C. K., Deol, H., Wagner, G. F., and DiMattia, G. E. (1998) Comparative analysis of mammalian stanniocalcin genes. *Endocrinology* **139,** 4714–4725
8. Chang, A. C., Cha, J., Koentgen, F., and Reddel, R. R. (2005) The murine stanniocalcin 1 gene is not essential for growth and development. *Mol. Cell. Biol.* **25,** 10604–10610
9. Chang, A. C., Hook, J., Lemckert, F. A., McDonald, M. M., Nguyen, M. A., Hardeman, E. C., Little, D. G., Gunning, P. W., and Reddel, R. R. (2008) The murine stanniocalcin 2 gene is a negative regulator of postnatal growth. *Endocrinology* **149,** 2403–2410
10. Sheikh-Hamad, D., Bick, R., Wu, G. Y., Christensen, B. M., Razeghi, P., Poindexter, B., Taegtmeyer, H., Wamsley, A., Padda, R., Entman, M., Nielsen, S., and Youker, K. (2003) Stanniocalcin-1 is a naturally occurring L-channel inhibitor in cardiomyocytes: relevance to human heart failure. *Am. J. Physiol. Heart Circ. Physiol.* **285,** H442-H448
11. Wagner, G. F., Vozzolo, B. L., Jaworski, E., Haddad, M., Kline, R. L., Olsen, H. S., Rosen, C. A., Davidson, M. B., and Renfro, J. L. (1997) Human stanniocalcin inhibits renal phosphate excretion in the rat. *J. Bone Miner. Res.* **12,** 165–171
12. Madsen, K. L., Tavernini, M. M., Yachimec, C., Mendrick, D. L., Alfonso, P. J., Buergin, M., Olsen, H. S., Antonaccio, M. J., Thomson, A. B., and Fedorak, R. N. (1998) Stanniocalcin: a novel protein regulating calcium and phosphate transport across mammalian intestine. *Am. J. Physiol.* **274,** G96-G102
13. Serlachius, M., and Andersson, L. C. (2004) Upregulated expression of stanniocalcin-1 during adipogenesis. *Exp. Cell Res.* **296,** 256–264
14. Wu, S., Yoshiko, Y., and De Luca, F. (2006) Stanniocalcin 1 acts as a paracrine regulator of growth plate chondrogenesis. *J. Biol. Chem.* **281,** 5120–5127
15. Chang, A. C., and Reddel, R. R. (1998) Identification of a second stanniocalcin cDNA in mouse and human: stanniocalcin 2. *Mol. Cell. Endocrinol.* **141,** 95–99
16. DiMattia, G. E., Varghese, R., and Wagner, G. F. (1998) Molecular cloning and characterization of stanniocalcin-related protein. *Mol. Cell. Endocrinol.* **146,** 137–140
17. Ishibashi, K., Miyamoto, K., Taketani, Y., Morita, K., Takeda, E., Sasaki, S., and Imai, M. (1998) Molecular cloning of a second human stanniocalcin homologue (STC2). *Biochem. Biophys. Res. Commun.* **250,** 252–258
18. Gagliardi, A. D., Kuo, E. Y., Raulic, S., Wagner, G. F., and DiMattia, G. E. (2005) Human stanniocalcin-2 exhibits potent growth-suppressive properties in transgenic mice independently of growth hormone and IGFs. *Am. J. Physiol. Endocrinol. Metab.* **288,** E92-E105
19. Jepsen, M. R., Kløverpris, S., Mikkelsen, J. H., Pedersen, J. H., Füchtbauer, E. M., Laursen, L. S., and Oxvig, C. (2015) Stanniocalcin-2 inhibits mammalian growth by proteolytic inhibition of the insulin-like growth factor axis. *J. Biol. Chem.* **290,** 3430–3439
20. Oxvig, C. (2015) The role of PAPP-A in the IGF system: location, location, location. *J. Cell Commun. Signal.* **9,** 177–187
21. Conover, C. A., Bale, L. K., Overgaard, M. T., Johnstone, E. W., Laursen, U. H., Füchtbauer, E. M., Oxvig, C., and van Deursen, J. (2004) Metalloproteinase pregnancy-associated plasma protein A is a critical growth

regulatory factor during fetal development. *Development* **131,** 1187–1194
22. Stewart, C. E., and Rotwein, P. (1996) Growth, differentiation, and survival: multiple physiological functions for insulin-like growth factors. *Physiol. Rev.* **76,** 1005–1026
23. Forbes, B. E., McCarthy, P., and Norton, R. S. (2012) Insulin-like growth factor binding proteins: a structural perspective. *Front. Endocrinol.* **3,** 38
24. Overgaard, M. T., Boldt, H. B., Laursen, L. S., Sottrup-Jensen, L., Conover, C. A., and Oxvig, C. (2001) Pregnancy-associated plasma protein-A2 (PAPP-A2), a novel insulin-like growth factor-binding protein-5 proteinase. *J. Biol. Chem.* **276,** 21849–21853
25. Boldt, H. B., Overgaard, M. T., Laursen, L. S., Weyer, K., Sottrup-Jensen, L., and Oxvig, C. (2001) Mutational analysis of the proteolytic domain of pregnancy-associated plasma protein-A (PAPP-A): classification as a metzincin. *Biochem. J.* **358,** 359–367
26. Overgaard, M. T., Oxvig, C., Christiansen, M., Lawrence, J. B., Conover, C. A., Gleich, G. J., Sottrup-Jensen, L., and Haaning, J. (1999) Messenger ribonucleic acid levels of pregnancy-associated plasma protein-A and the proform of eosinophil major basic protein: expression in human reproductive and nonreproductive tissues. *Biol. Reprod.* **61,** 1083–1089
27. Lawrence, J. B., Oxvig, C., Overgaard, M. T., Sottrup-Jensen, L., Gleich, G. J., Hays, L. G., Yates, J. R., 3rd, and Conover, C. A. (1999) The insulin-like growth factor (IGF)-dependent IGF binding protein-4 protease secreted by human fibroblasts is pregnancy-associated plasma protein-A. *Proc. Natl. Acad. Sci. U.S.A.* **96,** 3149–3153
28. Laursen, L. S., Overgaard, M. T., Søe, R., Boldt, H. B., Sottrup-Jensen, L., Giudice, L. C., Conover, C. A., and Oxvig, C. (2001) Pregnancy-associated plasma protein-A (PAPP-A) cleaves insulin-like growth factor binding protein (IGFBP)-5 independent of IGF: implications for the mechanism of IGFBP-4 proteolysis by PAPP-A. *FEBS Lett.* **504,** 36–40
29. Monget, P., Mazerbourg, S., Delpuech, T., Maurel, M. C., Manière, S., Zapf, J., Lalmanach, G., Oxvig, C., and Overgaard, M. T. (2003) Pregnancy-associated plasma protein-A is involved in insulin-like growth factor binding protein-2 (IGFBP-2) proteolytic degradation in bovine and porcine preovulatory follicles: identification of cleavage site and characterization of IGFBP-2 degradation. *Biol. Reprod.* **68,** 77–86
30. Varghese, R., Gagliardi, A. D., Bialek, P. E., Yee, S. P., Wagner, G. F., and Dimattia, G. E. (2002) Overexpression of human stanniocalcin affects growth and reproduction in transgenic mice. *Endocrinology* **143,** 868–876
31. Overgaard, M. T., Haaning, J., Boldt, H. B., Olsen, I. M., Laursen, L. S., Christiansen, M., Gleich, G. J., Sottrup-Jensen, L., Conover, C. A., and Oxvig, C. (2000) Expression of recombinant human pregnancy-associated plasma protein-A and identification of the proform of eosinophil major basic protein as its physiological inhibitor. *J. Biol. Chem.* **275,** 31128–31133
32. Gyrup, C., and Oxvig, C. (2007) Quantitative analysis of insulin-like growth factor-modulated proteolysis of insulin-like growth factor binding protein-4 and -5 by pregnancy-associated plasma protein-A. *Biochemistry* **46,** 1972–1980
33. Gyrup, C., Christiansen, M., and Oxvig, C. (2007) Quantification of proteolytically active pregnancy-associated plasma protein-A with an assay based on quenched fluorescence. *Clin. Chem.* **53,** 947–954
34. Godiksen, S., Soendergaard, C., Friis, S., Jensen, J. K., Bornholdt, J., Sales, K. U., Huang, M., Bugge, T. H., and Vogel, L. K. (2013) Detection of active matriptase using a biotinylated chloromethyl ketone peptide. *PLoS ONE* **8,** e77146
35. Oxvig, C., Sand, O., Kristensen, T., Kristensen, L., and Sottrup-Jensen, L. (1994) Isolation and characterization of circulating complex between human pregnancy-associated plasma protein-A and proform of eosinophil major basic protein. *Biochim. Biophys. Acta* **1201,** 415–423
36. Qin, Q. P., Christiansen, M., Oxvig, C., Pettersson, K., Sottrup-Jensen, L., Koch, C., and Nørgaard-Pedersen, B. (1997) Double-monoclonal immunofluorometric assays for pregnancy-associated plasma protein A/proeosinophil major basic protein (PAPP-A/proMBP) complex in first-trimester maternal serum screening for Down syndrome. *Clin. Chem.* **43,** 2323–2332
37. Laursen, L. S., Kjaer-Sorensen, K., Andersen, M. H., and Oxvig, C. (2007) Regulation of insulin-like growth factor (IGF) bioactivity by sequential proteolytic cleavage of IGF binding protein-4 and -5. *Mol. Endocrinol.* **21,** 1246–1257
38. Trindade, D. M., Silva, J. C., Navarro, M. S., Torriani, I. C., and Kobarg, J. (2009) Low-resolution structural studies of human Stanniocalcin-1. *BMC Struct. Biol.* **9,** 57
39. Hulova, I., and Kawauchi, H. (1999) Assignment of disulfide linkages in chum salmon stanniocalcin. *Biochem. Biophys. Res. Commun.* **257,** 295–299
40. Zhang, J., Alfonso, P., Thotakura, N. R., Su, J., Buergin, M., Parmelee, D., Collins, A. W., Oelkuct, M., Gaffney, S., Gentz, S., Radman, D. P., Wagner, G. F., and Gentz, R. (1998) Expression, purification, and bioassay of human stanniocalcin from baculovirus-infected insect cells and recombinant CHO cells. *Protein Expr. Purif.* **12,** 390–398
41. Roch, G. J., and Sherwood, N. M. (2011) Stanniocalcin has deep evolutionary roots in eukaryotes. *Genome Biol. Evol.* **3,** 284–294
42. Brew, K., and Nagase, H. (2010) The tissue inhibitors of metalloproteinases (TIMPs): an ancient family with structural and functional diversity. *Biochim. Biophys. Acta* **1803,** 55–71
43. Tseng, D. Y., Chou, M. Y., Tseng, Y. C., Hsiao, C. D., Huang, C. J., Kaneko, T., and Hwang, P. P. (2009) Effects of stanniocalcin 1 on calcium uptake in zebrafish (*Danio rerio*) embryo. *Am. J. Physiol. Regul. Integr. Comp. Physiol.* **296,** R549-R557
44. Lin, C. H., Su, C. H., and Hwang, P. P. (2014) Calcium-sensing receptor mediates Ca^{2+} homeostasis by modulating expression of PTH and stanniocalcin. *Endocrinology* **155,** 56–67
45. Dai, W., Bai, Y., Hebda, L., Zhong, X., Liu, J., Kao, J., and Duan, C. (2014) Calcium deficiency-induced and TRP channel-regulated IGF1R-PI3K-Akt signaling regulates abnormal epithelial cell proliferation. *Cell Death Differ.* **21,** 568–581
46. Kjaer-Sorensen, K., Engholm, D. H., Kamei, H., Morch, M. G., Kristensen, A. O., Zhou, J., Conover, C. A., Duan, C., and Oxvig, C. (2013) Pregnancy-associated plasma protein A (PAPP-A) modulates the early developmental rate in zebrafish independently of its proteolytic activity. *J. Biol. Chem.* **288,** 9982–9992
47. Pollak, M. (2012) The insulin and insulin-like growth factor receptor family in neoplasia: an update. *Nat. Rev. Cancer* **12,** 159–169
48. Mikkelsen, J. H., Resch, Z. T., Kalra, B., Savjani, G., Kumar, A., Conover, C. A., and Oxvig, C. (2014) Indirect targeting of IGF receptor signaling *in vivo* by substrate-selective inhibition of PAPP-A proteolytic activity. *Oncotarget* **5,** 1014–1025
49. Becker, M. A., Haluska, P., Jr., Bale, L. K., Oxvig, C., and Conover, C. A. (2015) A novel neutralizing antibody targeting pregnancy-associated plasma protein-A inhibits ovarian cancer growth and ascites accumulation in patient mouse tumorgrafts. *Mol. Cancer Ther.* **14,** 973–981
50. Peña, C., Céspedes, M. V., Lindh, M. B., Kiflemariam, S., Mezheyeuski, A., Edqvist, P. H., Hägglöf, C., Birgisson, H., Bojmar, L., Jirström, K., Sandström, P., Olsson, E., Veerla, S., Gallardo, A., Sjöblom, T., Chang, A. C., Reddel, R. R., Mangues, R., Augsten, M., and Ostman, A. (2013) STC1 expression by cancer-associated fibroblasts drives metastasis of colorectal cancer. *Cancer Res.* **73,** 1287–1297
51. Welcsh, P. L., Lee, M. K., Gonzalez-Hernandez, R. M., Black, D. J., Mahadevappa, M., Swisher, E. M., Warrington, J. A., and King, M. C. (2002) BRCA1 transcriptionally regulates genes involved in breast tumorigenesis. *Proc. Natl. Acad. Sci. U.S.A.* **99,** 7560–7565
52. Chang, A. C., Doherty, J., Huschtscha, L. I., Redvers, R., Restall, C., Reddel, R. R., and Anderson, R. L. (2015) STC1 expression is associated with tumor growth and metastasis in breast cancer. *Clin. Exp. Metastasis* **32,** 15–27
53. Loddo, M., Andryszkiewicz, J., Rodriguez-Acebes, S., Stoeber, K., Jones, A., Dafou, D., Apostolidou, S., Wollenschlaeger, A., Widschwendter, M., Sainsbury, R., Tudzarova, S., and Williams, G. H. (2014) Pregnancy-associated plasma protein A regulates mitosis and is epigenetically silenced in breast cancer. *J. Pathol.* **233,** 344–356
54. Moore, E. E., Kuestner, R. E., Conklin, D. C., Whitmore, T. E., Downey, W., Buddle, M. M., Adams, R. L., Bell, L. A., Thompson, D. L., Wolf, A., Chen, L., Stamm, M. R., Grant, F. J., Lok, S., Ren, H., and De Jongh, K. S. (1999) Stanniocalcin 2: characterization of the protein and its localization to human pancreatic alpha cells. *Horm. Metab. Res.* **31,** 406–414